

Analytical Closed-Form Investigation of PWM Inverter Induction-Motor Drive Performance under DC-Bus Voltage Pulsation

JIRI KLIMA

Department of Electrical Engineering and Automation
Faculty of Engineering in CZUon Prague
CZECH REPUBLIC

Abstract—This paper presents an analytical closed-form mathematical model and analysis of the influence of the DC-bus ripple voltage of the three-phase voltage source inverter (VSI) with the space-vector PWM (SVPWM) on the induction machine phase voltages, currents and torque pulsations. The analytical expressions for the voltage and current space-vectors as a function of the dc-bus voltage pulsation are derived. Using superposition we can determine the separate parts of the motor currents. Next, it is shown, that dc-link voltage ripple components may cause large torque pulsation. The proposed analytical method is based on the mixed p-z approach, enabling presentation of the results in lucid and closed-form. To verify the effectiveness of the proposed analytical model, experimental results based on laboratory setup were obtained.

Key-Words: Induction Motor, Analytical Model, Pulse Width Modulation, Voltage Source Inverter

1 Introduction

As it was shown [1], the unbalance conditions in the three-phase input line voltages may cause the rectifier stage to enter single-phase rectifier operation. This situation can create significant voltage harmonic in the dc bus at twice the line frequency (100 Hz for 50 Hz supply.)

This dc bus voltage ripple affects the PWM output voltage waveforms, causing low frequency harmonic currents to flow into the motor.

An increase in electric losses, excessive rise of the motor temperature, appearance of the torque pulsation, and noise problems as well as the dc-bus capacitor stress are just some of the possible problems [7], [9]. So, the analysis of the dc-link voltage pulsation and its influence on the motor performances is of great importance.

The dc-bus voltage pulsation is composed of several sources such as follows [3]:

- a) The diode rectification of the AC line voltage causes pulsation components [1]
- b) Unbalance in the AC power supply generates 100 or 120-Hz component [3]
- c) In some faulty conditions in the front-end rectifier dc link voltage may consist again pulsation [2]
- d) Transient voltage sags in the three-phase input line voltages can cause the rectifier stage to enter single-phase rectifier operation with corresponding dc-bus voltage pulsation [4].

This paper presents a mathematical model which enables us to solve both the steady-state and transient-state performance of the three-phase VSI under dc-link voltage ripple feeding an induction motor and respecting the real PWM inverter voltage. The analytical closed form solution makes use of the Laplace and modified Z-transforms of the space vectors (mixed p-z approach [12], [13]). From the Laplace transform of the stator voltage vectors we can also derive Fourier series to predict the voltage harmonic spectra.

Analysis is made under the assumption that the motor runs at a constant speed. The electromechanical time constant is much larger than the electrical ones and, therefore, it is reasonable to assume that the rotor speed remains constant during a sampling period.

The attention is focused on the calculation of the closed-form expressions for the stator and rotor currents. From these equations an analytical expression for the electromagnetic torque in dependence of the dc-link pulsation is derived. Torque ripple deteriorates the static and dynamic characteristics of induction motors and it may become an important issue in induction motor design. It may cause mechanical oscillations, which are particularly dangerous in resonant frequencies of the load. Moreover, torque ripple leads to an increase of the motor noise. Particularly the appearance of the sixth torque harmonic was observed by many researchers [10] [11]. But in this paper it will be shown that the dc-link ripple voltage components may give rise to an additional large torque ripple component.

The paper contributes to a better understanding of the effects of dc link voltage ripple conditions on operation of an induction machine by providing closed-form

expressions both in time and frequency domain, taking into account the real PWM waveforms. In particular, this mathematical model provides a useful tool for the development of the dc link ripple mitigation technique by a proper modulation technique of the inverter. The proposed mathematical model has also been verified by experiment. The experiments were provided both in six-step and space-vector PWM (SVPWM) regimes. Experimental results show good agreement with theoretical prediction.

2 Stator Voltage-Space Vectors

A simplified scheme of the system is shown in Fig.1. Three-phase ac line voltages are fed to a three-phase rectifier bridge. The dc choke inductance has value L_{dc} . The dc bus voltage is buffered by the two dc bus capacitances C . The output part is composed of the PWM inverter consisting of six IGBT switches and their antiparallel diodes. The PWM voltage waveforms are delivered to the induction machine following a constant volts-per-hertz algorithm.

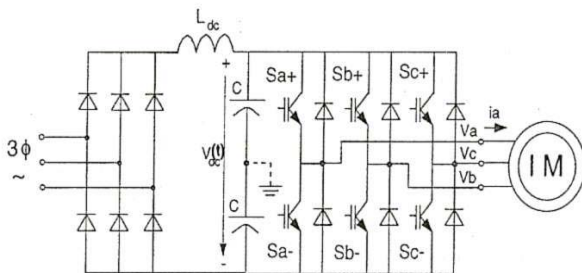


Fig.1. Rectifier-inverter induction motor drive

This paper is focused primarily with the output part of the drive. This approach takes into account the dc-link voltage ripple, due to the finite dc link capacitors. It has been shown [1] that the input rectifier stage of the system shown in Fig.1 can easily slip into single-phase operation during input line voltage sag or/and unbalance conditions. The dominant ac component in the dc bus voltage ripple occurs at the second line harmonic frequency (100 Hz).

We assume that dc link voltage contains both the constant and pulsation parts that may be expressed as:

$$V_{dc}(t) = V_{dc0} + \sum_{i=1}^{\infty} \Delta V_{dci} \cos(i2\omega_1 t + \psi_i) \quad (1a)$$

The voltage ripple appearing across the dc link capacitor terminals contains, only even-order harmonics [2].

The dominant ac frequency component that appears in the dc link voltage pulsates at twice the excitation frequency ($2f_1$).

As a result for the closed-form mathematical solution, we suppose as in [1], that the dc link voltage can be approximated by the constant average value V_{dc} and pulsation part $\Delta V_{dc} \cos 2\omega_1 t$, where

ω_1 is an angular frequency of the supply voltage ($2\pi 50$ or $2\pi 60, s^{-1}$).

But if needed we can take into consideration also the next higher harmonics with the angular frequency $4\omega_1$.

The switching elements will be considered as ideal switches. We also assume constant rotor speed and linear parameters of the motor.

As the dominant ac component in the resulting dc bus voltage $V_{dc}(t)$ is created by the second-harmonic voltage component it also dominates in generation of undesirable effects in the induction-machine operating performance characteristics. Next, attention is focused on developing the closed-form mathematical model that quantifies the induction-machine performance effects caused by this second-harmonic voltage component.

The stator voltage space vector can be expressed in the complex $\alpha\beta$ plane with respect to $\pi/3$ symmetry as follows:

$$V(n, \varepsilon) = (V_{dc} + \Delta V_{dc}) \cos(2\omega_1(n + \varepsilon)T) \frac{2}{3} e^{j\omega_0 T n} \quad (1b)$$

where

$\omega_0 = \frac{2\pi}{T_0}$ is the inverter output fundamental angular frequency.

In (1b) time is expressed in per units as

$$t = (n + \varepsilon)T = (n + \varepsilon) \frac{T_0}{6} \quad (2)$$

where $T = T_0/6$ is a sector period, n is a number of a sector and ε is a per unit time inside sector T .

$$0 \leq \varepsilon \leq 1 \quad (2a)$$

To express the voltage space vector with SVPWM we must include in (1b) also the modulation function and the stator voltage vector is calculated as follows:

$$\begin{aligned}
 V(n, \varepsilon) &= \frac{[V_{dc} + \Delta V_{dc} \cos 2\omega_1(n + \varepsilon)T]}{3} 2e^{jn\frac{\pi}{3}} \sum_k f(\varepsilon, k) e^{j\pi\frac{\alpha_k}{3}} = \\
 &= \frac{2}{3} V_{dc} e^{jn\frac{\pi}{3}} \sum_k f(\varepsilon, k) e^{j\pi\frac{\alpha_k}{3}} + \\
 &\frac{2}{3} \Delta V_{dc} \cos[2\omega_1(n + \varepsilon)T] e^{jn\frac{\pi}{3}} \sum_k f(\varepsilon, k) e^{j\pi\frac{\alpha_k}{3}} = V_d(n, \varepsilon) + V_p(n, \varepsilon)
 \end{aligned} \quad (3)$$

In (3) $V_d(n, \varepsilon)$ is the voltage space vector created from the smooth part of the dc bus voltage (V_{dc}), and $V_p(n, \varepsilon)$ is the voltage space vector caused by the second-harmonic voltage component (ΔV_{dc}).

and

$\sum_k f(\varepsilon, k) e^{j\pi\frac{\alpha_k}{3}}$ is the modulation function given by the switching instants within the k-th pulse. This function contains both time and phase vector dependency. Time dependency is given as follows:

$$f(\varepsilon, k) = 1, \text{ for } \dots \varepsilon_{kA} \leq \varepsilon \leq \varepsilon_{kB} \quad ,$$

$$f(\varepsilon, k) = 0 \quad \text{else} \quad (3a)$$

where: ε_{kA} is start point setting per unit time of the k-th pulse

ε_{kB} is end point setting per unit time of the k-th pulse

pulse

the duty ratio switching time is :

$$\Delta \varepsilon_k = \varepsilon_{kB} - \varepsilon_{kA} \quad (3b)$$

The expressions for the switching times in the normal SVPWM are given in [9].

Phase dependency is given by the function

$$g(k) = e^{j\pi\frac{\alpha_k}{3}} \quad (3c)$$

Where α_k shows which voltage vector is used in the k-th pulse .

For the conventional space-vector PWM (CSVPWM) where two adjacent space vectors within a sampling period are used, α_k can be 0 or 1 (i.e. voltage vectors in n-th sector period can have direction

$$e^{j\frac{\pi}{3}n} e^{j\frac{\pi}{3}0} = e^{j\frac{\pi}{3}n}, \text{ and } e^{j\frac{\pi}{3}n} e^{j\frac{\pi}{3}1} = e^{j\frac{\pi}{3}(n+1)})$$

In the first sector during the first two sampling periods the following voltage vector sequence is used:

$(V_0 - V_1 - V_2 - V_7), (V_7 - V_2 - V_1 - V_0)$, where V_0 and V_7 are the zero voltage vectors.

With regard to the voltage vector sequences within the first switching period (the two sampling periods), we can define α_k as follows:

$$\alpha_{2m-1} = \frac{1 + (1)^m}{2}, \alpha_{2m} = \frac{1 + (1)^{m+1}}{2} \quad (3d)$$

m is a number of sampling period

The trajectory of $V(n, \varepsilon)$ in the complex $\alpha\beta$ plane for $\Delta V_{dc} = 0.05$, and $f_0 = f_1 = 50\text{Hz}$, $f_{sw} = 3000\text{Hz}$ is shown in Fig.2

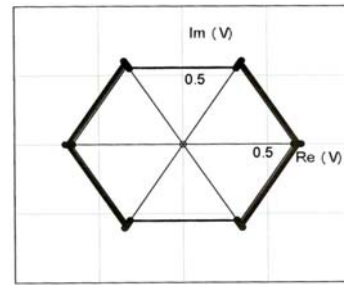


Fig.2 Voltage space vector trajectory with dc-link pulsation component $\Delta V_{dc} = 0.05$

Using well known formula for cosine function

$$\cos x = \frac{e^{jx} + e^{-jx}}{2} \quad (4)$$

we can write for the pulsating part in (3)

$$V_p(n, \varepsilon) = \frac{\Delta V_{dc}}{3} e^{j2\omega_1 T(n + \varepsilon)} e^{jn\frac{\pi}{3}} \sum_k f(\varepsilon, k) e^{j\pi\frac{\alpha_k}{3}} +$$

$$\frac{\Delta V_{dc}}{3} e^{-j2\omega_1 T(n + \varepsilon)} e^{jn\frac{\pi}{3}} \sum_k f(\varepsilon, k) e^{j\pi\frac{\alpha_k}{3}} = V_{pp}(n, \varepsilon) + V_{pn}(n, \varepsilon) \quad (5)$$

From (5) it may be seen that pulsation part of the voltage space vector $V_p(n, \varepsilon)$ may be resolved into two

components: the positive sequence $V_{pp}(n, \varepsilon)$, and the negative sequence: $V_{pn}(n, \varepsilon)$

The trajectories of the both parts in the complex plane for the same operating conditions as used to calculate trajectory in Fig.2, are shown in Fig.3

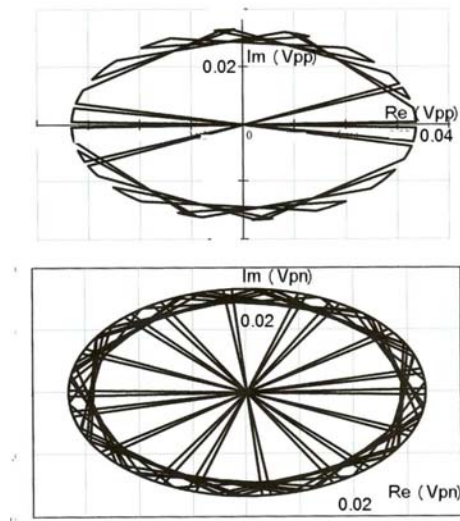


Fig. 3 Trajectories of two parts creating voltage space vector with dc link pulsation component $\Delta V_{dc} = 0.05$

3 Closed-Form Analytical Model

3.1 Induction-Machine Circuit Analysis

Using the mixed p-z approach as shown in [12], [13] we can derive the closed-form analytical expressions for the stator and/or rotor currents and also for the electromagnetic torque.

From these relations we can estimate the influence of the dc link voltage pulsation on the currents and electromagnetic torque waveforms.

First, we can derive the Laplace transform of the symmetrical voltage vector sequences (3). For this, we can use the relation between the Laplace and modified Z transforms [13].

Using (2) and its derivation $dt = Td\varepsilon$ we can derive the Laplace transforms of the periodic waveform as:

$$V(p) = \sum_{n=0}^{\infty} \left(\int_0^1 V(n, \varepsilon) e^{-p(n+\varepsilon)T} T d\varepsilon \right) = T \int_0^1 V(z, \varepsilon) e^{-pT\varepsilon} d\varepsilon \quad (6)$$

where: $z = e^{pT}$, and

$$V(z, \varepsilon) = \sum_{n=0}^{\infty} V(n, \varepsilon) z^{-n} \quad (7)$$

$V(z, \varepsilon)$ is the modified Z transform of $V(n, \varepsilon)$.

Substituting (3) into (6) with the use of the Z transform of exponential functions we can find the Laplace transform of the stator voltage vector as follows:

$$\begin{aligned} V_1(p) = & \frac{2}{3} V_{dc} \frac{1}{p} \frac{e^{pT}}{e^{pT} - e^{j\frac{\pi}{3}}} \sum_k (e^{-pT\varepsilon_{kA}} - e^{-pT\varepsilon_{kB}}) + \\ & \frac{1}{3} \Delta V_{dc} \frac{1}{p-2j\omega_1} \frac{e^{pT}}{e^{pT} - e^{j(\frac{\pi}{3}+2\omega_1 T)}} \sum_k (e^{-T\varepsilon_{kA}(p-2j\omega_1)} - e^{-T\varepsilon_{kB}(p-2j\omega_1)}) + \\ & \frac{1}{3} \Delta V_{dc} \frac{1}{p+2j\omega_1} \frac{e^{pT}}{e^{pT} - e^{j(\frac{\pi}{3}-2\omega_1 T)}} \sum_k (e^{-T\varepsilon_{kA}(p+2j\omega_1)} - e^{-T\varepsilon_{kB}(p+2j\omega_1)}) = \\ & V_0(p) + V_{IP}(p-2j\omega_1) + V_{IN}(p+2j\omega_1) \end{aligned} \quad (8)$$

Equation (8) is the Laplace transform of the stator voltage vector, respecting the influence of the dc-link voltage ripple. It contains three parts. The first term is the Laplace transform of the stator voltage vector with constant value in the dc link voltage. The last two terms are the Laplace transform of the positive and the negative ripple components of the dc link voltage.

When we know the Laplace transform of the stator voltage vectors we can derive the Laplace transform of the motor current vectors. In order to calculate the motor current space vectors, it is convenient to carry out the analysis in the stator reference frame.

From the motor equations in the stator reference frame we can derive the Laplace transform of the stator and rotor currents, respectively as follows

$$\begin{aligned} I_s(p) = V_1(p) \frac{A_s(p)}{B_s(p)} = V_1(p) \frac{k_R + p - j\omega}{\sigma L_s (p - p_1)(p - p_2)} \\ I_r(p) = V_1(p) \frac{A_r(p)}{B_r(p)} = -V_1(p) \frac{L_m (p - j\omega)}{\sigma L_s L_r (p - p_1)(p - p_2)} \end{aligned} \quad (9)$$

In the foregoing equations, R_s is the stator resistance, R_r the rotor resistance, L_s the stator self-inductance, L_r the rotor self-inductance, L_m is the mutual inductance, and ω the rotor electrical angular velocity

$$\sigma = 1 - L_m^2 / (L_s L_r), \quad k_s = R_s / L_s, \quad k_r = R_r / L_r,$$

and $p_{1,2}$ in (9) are the roots of the characteristic equation: $B(p) = 0$, that are given as follows:

$$p_{1,2} = \frac{-(k_S + k_R - j\sigma\omega)}{2\sigma} \pm \sqrt{\left(\frac{k_S + k_R - j\sigma\omega}{2\sigma}\right)^2 + \frac{j\omega k_S - k_S k_R}{\sigma}} \quad (10)$$

The inverse Laplace transform of (9) cannot be solved directly using the residue theorem, as (9) contains infinite numbers of poles given by the following equations (see eq.(8)):

$$\begin{aligned} e^{j\frac{\pi}{3}} - e^{pT} &= 0 \\ e^{j(\frac{\pi}{3}-2\omega_1 T)} - e^{pT} &= 0, \quad e^{j(\frac{\pi}{3}+2\omega_1 T)} - e^{pT} = 0 \end{aligned} \quad (11)$$

The solution of the time dependency of the motor current vectors can be found in the closed form as presented in [14].

If we use the Heaviside theorem

$$L^{-1}\left\{\frac{A(p)}{pB(p)}\right\} = \frac{A(0)}{B(0)} + \sum_k \frac{A(p_k)}{p_k B'(p_k)} e^{p_k T} \quad (12)$$

and also the formula for multiplication by an exponential function

$$L\left\{e^{j\omega T} f(t)\right\} = F(p - j\omega T) \quad (13)$$

where $B'(p_k) = (dB/dp)_{p=p_k}$ and symbols $L\{\}$ and $L^{-1}\{\}$ mean the direct and inverse Laplace transforms, respectively, we can transform the formulas for the motor currents (9) from the Laplace into the modified Z-domain [13]. After doing that, we can use the residue theorem in the modified Z-transform to find the analytical closed-form solution both for the stator and for the rotor current vectors. The solution contains both the steady-state and transient components. As our attention is focused on the steady-state solution, applying superposition, the stator and rotor currents will have the closed-form solution shown in (14), for $n \rightarrow \infty$,

$$\begin{aligned} I_y(n, \varepsilon) &= I_y^1(0) e^{j\frac{\pi}{3}(n+1)} + \sum_{k=1}^2 I_y^1(p_k) e^{j\frac{\pi}{3}(n+1)} e^{p_k T \varepsilon} + \\ &I_y^2(2j\omega_1) e^{j\frac{\pi}{3}(n+1)} e^{2j\omega_1 T(n+\varepsilon)} + \\ &\sum_{k=1}^2 I_y^2(p_k - 2j\omega_1) e^{j(\frac{\pi}{3}+2\omega_1 T)(n+1)} e^{p_k T \varepsilon} + I_y^3(-2j\omega_1) e^{j\frac{\pi}{3}(n+1)} e^{-2j\omega_1 T(n+\varepsilon)} + \\ &\sum_{k=1}^2 I_y^3(p_k + 2j\omega_1) e^{j(\frac{\pi}{3}-2\omega_1 T)(n+1)} e^{p_k T \varepsilon} = \\ &I_{y0}(n, \varepsilon) + I_{yp}(n, \varepsilon) + I_{yn}(n, \varepsilon) \end{aligned} \quad (14)$$

where subscripts in (14) mean:

y is S (for the stator values) or y is R (for the rotor values), 0 are parts of (14) that are not dependent on angular frequency ω_1 , p means a positive sequence terms (depending on ω_1) and n means a negative sequence terms (depending on $-\omega_1$).

Similarly to (8) the overall steady-state stator/rotor currents contain three parts (terms arising from constant, positive and negative bus voltages, respectively).

These components are shown in Fig.4 for the pulsation of the dc bus 5%. The upper plot of Fig.4 shows current space-vector trajectory from the constant dc bus voltage, the middle and bottom plots show, respectively, current space-vector trajectory from the positive and negative dc bus voltage components. Fig.5 shows the induction machine stator phase currents, again for $f_1=f_0=50$ Hz, and the ac ripple voltage $\Delta V_{dc}=0.05$. As it will be shown in the section concerning with the frequency-domain analysis, the currents contain harmonics with frequencies 150 Hz (positive-sequence third harmonic component) and -50 Hz, (negative-sequence fundamental component), respectively. These harmonics cause the unbalance stator phase current waveforms as seen in Fig.5.

Owing to the dc bus voltage pulsation, the phase currents are distorted.

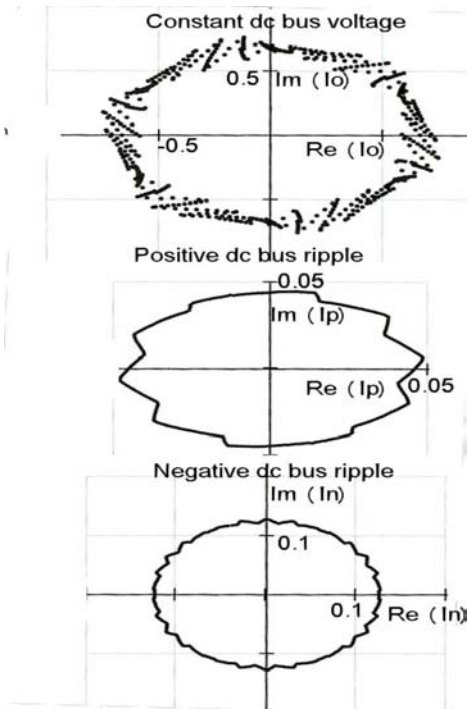


Fig.4 Closed-form analysis results of machine stator current vectors. $\Delta V_{dc} = 0.05$. Trajectories of the stator-current vectors.

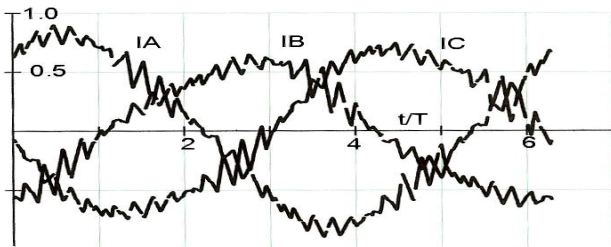


Fig.5 Closed-form analysis results of machine phase currents, $\Delta V_{dc} = 0.05$.

3.2 Electromagnetic Torque

Torque ripple with low frequency may become an important issue in induction motor drives. It causes mechanical oscillations, which are particularly dangerous in resonance frequencies of the system [12]. This torque ripple is usually superimposed to the torque ripple of switching frequency. Since the switching frequency has usually high value, its effect will be

suppressed by the electrical and mechanical damping of the motor and of the gear.

In steady state, along with an expected torque ripple of switching frequency, a superimposed pulsation was observed. Particularly, the appearance of the sixth torque harmonic was observed by many researchers [12], [10].

As it was shown in [10] the occurrence of zero vector intervals in PWM influences torque ripple, and leads to a sixth-order torque harmonics. But as it will be shown in the following part of this paper, the dc-bus voltage pulsation with angular frequency $2\omega_1$ may cause large torque pulsation with the same angular frequency.

The electromagnetic torque is given from the stator and rotor vector current by the following formula:

$$T_i(n, \epsilon) = \frac{3}{2} L_m \frac{P}{2} \text{Re} \{ j I_s^*(n, \epsilon) \cdot I_r(n, \epsilon) \} \quad (15)$$

where symbol * means complex conjugate value and P is the number of poles.

The expression for the complex stator and rotor currents in (14) can be used to develop an expression for the product in (15) as follows:

$$\begin{aligned} T_i(n, \epsilon) &= \frac{3}{2} L_m \frac{P}{2} \text{Re} \{ j I_{S0}^*(n, \epsilon) \cdot I_{R0}(n, \epsilon) \} + \\ &+ \frac{3}{2} L_m \frac{P}{2} \text{Re} \{ j (I_{Sp}^*(n, \epsilon) + I_{Sn}^*(n, \epsilon)) I_{R0}(n, \epsilon) \} + \\ &+ \frac{3}{2} L_m \frac{P}{2} \text{Re} \{ j I_{S0}^*(n, \epsilon) (I_{Rp}(n, \epsilon) + I_{Rn}(n, \epsilon)) \} + \\ &+ \frac{3}{2} L_m \frac{P}{2} \text{Re} \{ j (I_{Sp}^*(n, \epsilon) + I_{Sn}^*(n, \epsilon)) (I_{Rp}(n, \epsilon) + I_{Rn}(n, \epsilon)) \} \\ &= T_{i0}(n, \epsilon) + T_{i1}(n, \epsilon) + T_{i2}(n, \epsilon) + T_{iC}(n, \epsilon) \end{aligned} \quad (16)$$

This expression shows that, under unbalance input voltage conditions, the electromagnetic torque contains the following terms:

$T_{i0}(n, \epsilon)$ is the electromagnetic torque without dc bus ripple component. It contains an average dc term and sixth-harmonic pulsations caused by the inverter switching frequency.

$T_{i1}(n, \epsilon)$ and $T_{i2}(n, \epsilon)$ represent the products of the complex conjugate stator currents, which form the constant (ripple) dc bus and the complex rotor currents from the ripple (constant) dc bus voltage.

$T_{iC}(n, \epsilon)$ is the electromagnetic torque component from stator and rotor dc link pulsation parts. It has negligible value and we may put $T_{iC}(n, \epsilon) = 0$.

The separated torque components can be seen from Fig.6.

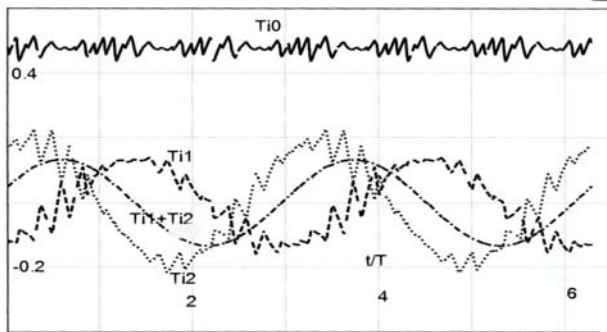


Fig.6 Closed-form analysis results of electromagnetic torque and its components.

Solid line- is the overall pulsation torque ($T_{iPUL}(n,\epsilon)$), dashed line-first is the pulsation component ($T_{i1}(n,\epsilon)$), dotted line is the second pulsation component ($T_{i2}(n,\epsilon)$). And the dash dotted line is the overall pulsation component ($T_{i1}(n,\epsilon)+ T_{i2}(n,\epsilon)$), $f_0=f_1=50$ Hz, $f_{sw}=3000$ Hz, $\Delta V_{dc} = 0.05$

From Fig.6 we can see that the overall pulsating electromagnetic torque can be expressed as follows:

$$T_{iPUL}(n,\epsilon) = T_{i1}(n,\epsilon) + T_{i2}(n,\epsilon) = A_T \cdot \sin(2 \cdot \omega_0 \cdot (n+\epsilon)T + \psi) \quad (17)$$

where A_T is an amplitude of the pulsating torque component (in Fig.6 we have $A_T=0.073$ p-u.) and ψ is a phase angle (in Fig.6 we have $\psi=8.3^\circ$).

As can be seen from Fig.6, both electromagnetic components forming the pulsation part have opposite direction and their sum is the pulsating waveform with the sine time dependency (without any high frequency ripple). The frequency of the pulsation is given by the frequency of dc bus voltage pulsation $2\omega_1$.

4 Experimental Verification

The analytical results and experimental waveforms for the sake of comparison are presented. All the analytical results were visualized from the derived equations by the program MATHCAD.

Experimental tests have been carried out using 1.1-kW 400-V, 50-Hz induction machine mounted on a laboratory ac dynamometer.

First, the comparison is made for the case of square-waveforms (without modulation) as in this case we can see the most pronounced influence of the dc link voltage ripple. The current waveforms in Fig.7 for 5% dc link voltage ripple and slip $s=0.6$, show the same features both for the experiments and closed-form analytical results. From the top to bottom we can see: i) analytical calculated phase voltage, ii) analytical calculated phase currents, iii) measured phase voltage and iv) measured phase currents.

Next comparison is made for the SVPWM waveforms.

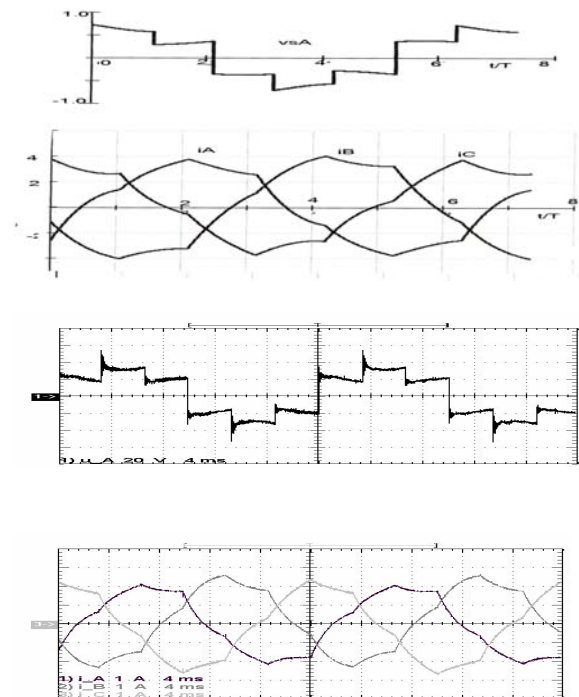


Fig.7 Closed-form analytical results and measured stator-current waveforms with dc bus voltage ripple $\Delta V_{dc} = 0.05$, slip $s=0.6$,

Fig.8 shows the measurement (upper and middle traces) and analytical calculated (bottom trace) results of the stator voltage and current waveforms for 5% pulsation with 4% motor slip.

The measurement and analytical calculated phase current waveforms for higher value of the ac pulsation (10%) and slip $s=4\%$ are shown in Fig.9. The measured current waveforms in Fig.9 show the same features as the calculated current waveform, including a high switching frequency ripple, providing further confirmation of the closed-form analytical results.

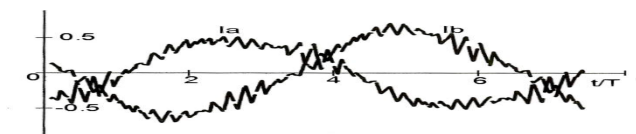
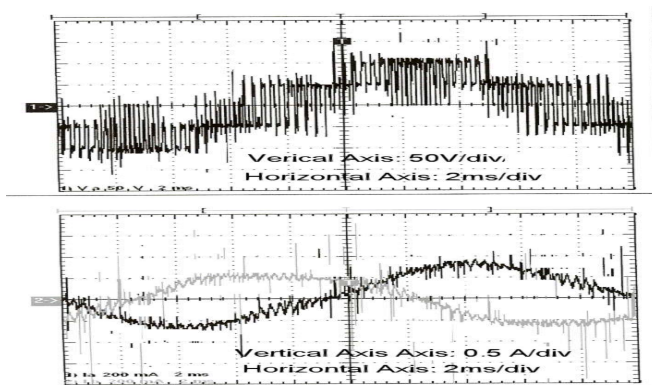


Fig.8 Measured phase voltage (upper trace), measured stator phase current (middle trace) and closed-form analytical results of machine stator phase currents with 5% ac link voltage ripple.

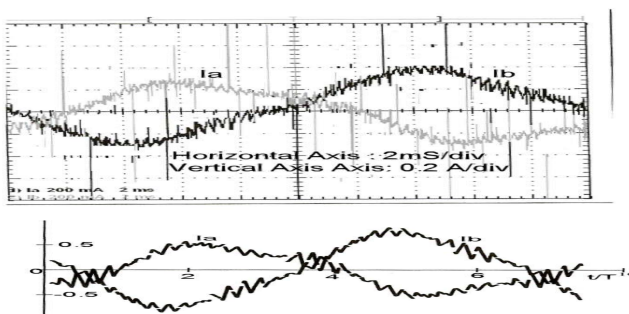


Fig.9 Measured (upper trace) stator-current waveforms with $\Delta V_{dc} = 0.1$. Closed-form (bottom trace) calculated stator-current waveforms.

5 Conclusion

Analytical analysis and mathematical closed-form model of three-phase voltage source PWM inverter fed induction motor drive under the dc-link ripple voltage component are presented in this paper. The analytical expressions for the voltage and current space-vectors as a function of the dc-link voltage pulsation are derived. By means of the modified Z-transform and the mixed p-z approach we can estimate the separate parts of the solution to estimate the influence of the dc link voltage pulsating on the current and torque waveforms.

The availability of the closed-form solution makes it possible to rapidly calculate the impact of the input unbalance conditions on the operating performance of an induction motor supplied from SVPWM voltage source inverter with finite value of dc-bus capacitance. Torque ripple produced in PWM inverter fed induction motor drives deteriorates both steady-state and dynamic characteristics of drives. It was found that dc-link ripple voltage components with angular frequency ω_0 may cause large torque pulsation with the same angular frequency. This torque ripple may be even dangerous at resonance frequencies of the system.

References:

- [1] Lee, K., Jahns, T.M., Berkopce, W.E., and Lipo, T.A., "Closed-form analysis of adjustable-speed drive performance under input-voltage unbalance and sag conditions," *IEEE Trans. Ind. Appl.*, vol.42, no. 3, May/June, 2006, pp.733-741
- [2] Chomat, M., and Schreier, L., "Compensation of Unbalanced Three-Phase Voltage Supply in Voltage Source Inverter." in *Proc. 28th Annual Conference of the IEEE Industrial Society*, 2002, pp.950-955
- [3] J. De Abreu, P.G., and Emanuel, A.E., "Induction motor thermal aging caused by voltage distortion and unbalance: Loss of useful life and its estimated cost." *IEEE Trans. Ind. Appl.*, vol 38, no 1, Jan/Feb 2000, pp.12-20,
- [4] Moran, L., Ziogas S.P., and Joos, G "Design aspects of synchronous PWM rectifier-inverter systems under unbalanced input voltage conditions." *IEEE Trans. Ind. Appl.*, vol 28, no 6, Nov/Dec 1992, pp.1286-1293,
- [5] Cross, A.M., and Evans, P.D., "DC link current in PWM inverters with unbalanced and non-linear loads." *IEE Proc. Electr. Pow. Appl.* Vo.143, No,6, 1999, pp.620-626
- [6] Chomat, M., and Schreier, L., "Control Method for DC-link Voltage Ripple Cancellation in Voltage Source Inverter Under Unbalanced Three-Phase Voltage Supply Conditions." *IEE Proc. Electric Power Appl.* Vol.152, Issue 3, May 2005, pp.494-500,
- [7] Broeck, H.W., and Skudelny, H-C., "Analytical Analysis of the Harmonic Effects of a PWM AC Drive." *IEEE Trans. Power Electron.* no.2, Mar./Apr. 1988, pp.216-222.
- [8] Broeck, H.W., and Wyk, J.D., "A Comparative Investigation of a Three-Phase Induction Machine Drive with a Component Minimised Voltage-Fed Inverter under Different Control Options," *IEEE Trans. Ind. Appl.*, Apr/Jun, 1984, pp.309-320

- [9] Andresen,E.C., and Haunt,A” Influence of the pulsewidth modulation control method on the performance of frequency inverter induction motor drives,” *European Trans.on Electric Power (ETEP)*, vol.3,1993,pp.151-161
- [10] Holtz,J., ”Identification and compensation of torque ripple in high-precision permanent magnet motor drives,” *IEEE Trans.Ind.Electron.*,vol.43,no.2,1996,pp.309-320
- [11] Hofmayer,,F.” Harmonic torque pulsation of induction machines-Analysis and compensation techniques using PWM inverters,” in Proceedings of *EPE Conference*, Toulouse, France,2003, pp.247-251
- [12] Klima,J.” Analytical Closed-Form Solution of a Space-Vector Modulated VSI Feeding an Induction Motor Drive. *IEEE Transaction on Energy Conversion*.Vol.17, No2.June,2002,pp.191-196
- [13] Klima,J.” Mixed p-z approach for time-domain analysis of voltage source inverters with periodic pulse width modulation.*IEEE Trans. on Circuits and Syst-II* vol.51,2004, no.10, pp.529-536